IEEE Photonics Journal
An IEEE Photonics Society Publication

Moiré-Based Interferometry for Magnification Calibration of Bitelecentric Lens System

Volume 7, Number 6, December 2015

Yi Zhou
Jiangping Zhu
Qinyuan Deng
Junbo Liu
Xinchun Si
Song Hu

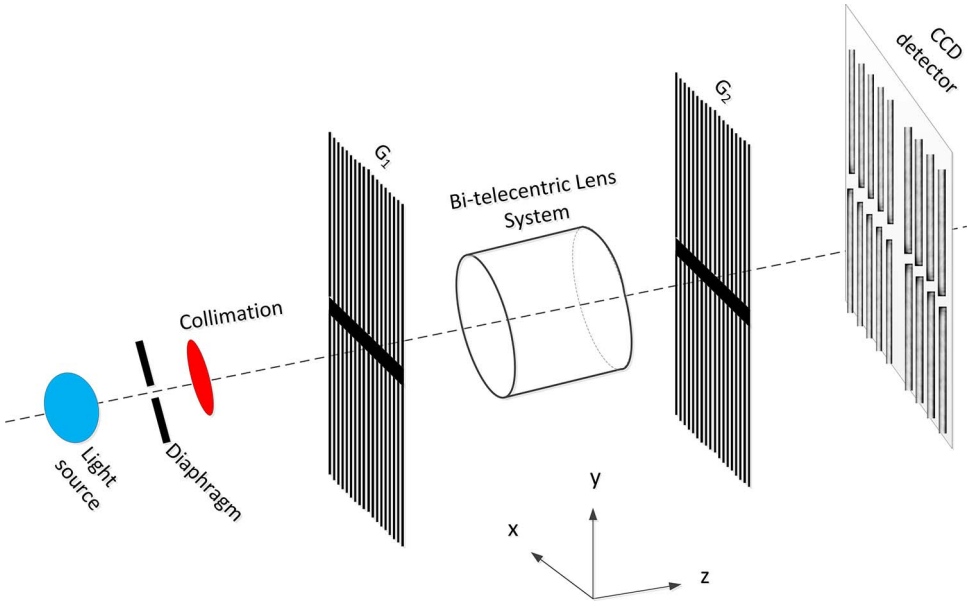

DOI: 10.1109/JPHOT.2015.2500892
1943-0655 © 2015 IEEE

Moiré-Based Interferometry for Magnification Calibration of Bitelecentric Lens System

Yi Zhou,[1,2] Jiangping Zhu,[3] Qinyuan Deng,[1,2] Junbo Liu,[1,2] Xinchun Si,[1,2] and Song Hu[1]

[1]State Key Laboratory of Optical Technologies for Microfabrication, Institute of Optics and Electronics, Chinese Academy of Sciences, Chengdu 610209, China
[2]University of Chinese Academy of Sciences, Beijing 100049, China
[3]School of Computer Science and Technology, Sichuan University, Chengdu 610064, China

DOI: 10.1109/JPHOT.2015.2500892

Manuscript received November 1, 2015; accepted November 11, 2015. Date of current version November 30, 2015. This work was supported by the Natural Science Foundation of China under Grant 61204114; by the Opening Project of State Key Laboratory of Polymer Materials Engineering, Sichuan University, under Grant 2015-4-28; and by the China Postdoctoral Science Foundation under Grant 2015M572472. Corresponding author: Y. Zhou (e-mail: alanzhouyi@163.com).

Abstract: The bitelecentric lens system is widely used in many domains, such as 3-D measurements and tube inspection. The magnification calibration for such a system is a crucial problem for its further application in achieving precise measurements. However, it is difficult to obtain an accurate result using a general magnification calibration method. In this paper, the Moiré-based interferometry is demonstrated to accurately calibrate the magnification of bitelecentric lens system that increases the speed and precision of the measurement. Two special grating marks containing upper and lower parts with slightly different periods are designed to generate Moiré fringes. By analyzing the finally obtained Moiré fringes, the magnification could be determined through Fourier-based phase analysis and a phase unwrapping algorithm, and the further the deviation is from the theoretical value, the more obvious the differences between upper and lower periods will be. Both simulations and experiments are conducted to verify the feasibility and effectiveness of the proposed approach. Results indicate that the magnification could be calibrated at the accuracy of 0.4% with extraordinary sensitivity.

Index Terms: Moiré fringes, magnification, grating marks, phase analysis.

1. Introduction

Because it has the unique characteristics of purely orthographic projections of scene points and maintaining a constant magnification over a specific range of object distances, the bi-telecentric lens system (BTLS) plays a significantly important role in the applied optics. BTLS, also characterized by high resolution, less distortion, and great magnification depth of field, has been extensively applied in dimensional-gauging applications like accurate 3-D measurements [1]–[3] and will be widely used in the non-gauging applications, mainly for inspection of tube or pipe bores and verification of hole clearance [4]–[6]. Magnification calibration of BTLS is an essential problem for its further applications in most applied optics such as 3-D measurement, microscope imaging, and inspection, but it is difficult to obtain accurate results by using the general methods if comparing the displayed size with its original one [7]–[10]. Imperatively, high-quality BTLS may have high resolution with little magnification distortion which seems to have no influence on application, it would

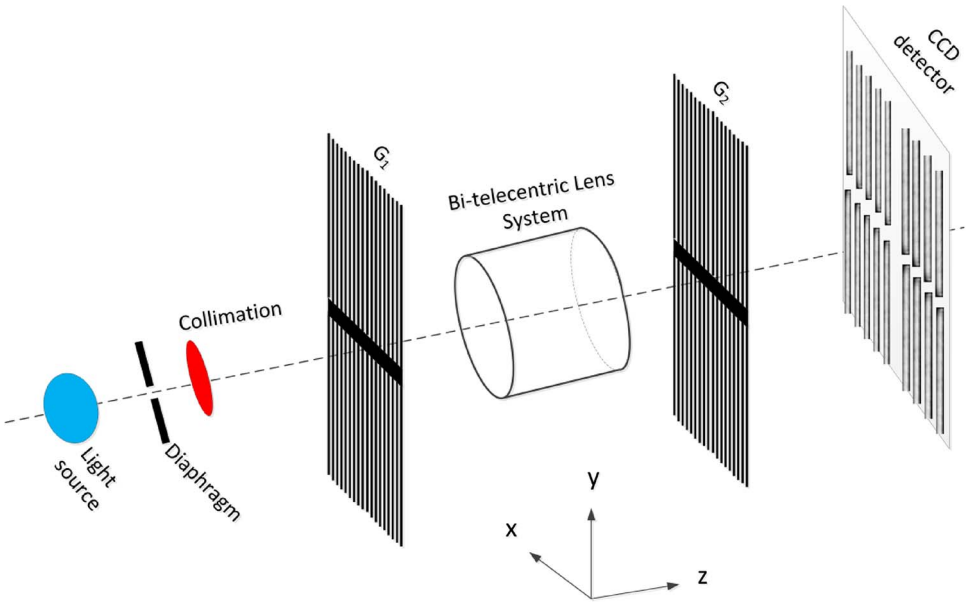

Fig. 1. Schematic of the moiré-based interferometry calibration. The whole setup consists of a light source, a diaphragm, a collimation, a referring grating G_1, BTLS (expected to be calibrated), an imaging grating G_2 and a CCD detector.

significantly result in unbearable measurement errors or even more severe in some applications, for example, microscope imaging and absolute profile measuring [11], [12]. The magnification distortion could not be neglected in almost every applied domain, thus the measurement of magnification is fairly critical and indispensable for its high-accuracy applications.

Some techniques for calibrating of magnification have been presented in the last few years. Traditionally, the magnification is evaluated by the simple pin method which seems not safe and inaccurate [13]. A Moiré fringe technique was also proposed for magnification checking by indicating the inclination of fringes [14]. As for widely used methods, Nakayama [15] proposed a novel calibration technique in which a multi-layer grating pattern was applied. And another effective method using replica specimens is also available in [16]. Nevertheless, it is still difficult to go into details of a determined calibrating technique. Moreover, above methods are not sensitive to evaluate the magnification and the accuracy of the methods also need to be improved for a higher stage. Evidently, for BTLS, magnification error is an intrinsic property which could not be totally eliminated; thus, it is meaningful and crucial to calibrate the exact value faster, simpler, more precise and more sensitive.

This paper proposes a Moiré-based interferometry method for calibrating the magnification of BTLS. Benefiting from its high sensitivity, pattern visualization, conveniences in image processing and frequency domain analysis, the Moiré-based method could evaluate the magnification steadier and more convenient with raised sensitivity [17]–[21]. The theory of this Moiré-based method is briefly discussed, and analysis models of the Moiré fringes which occur in the two superposed gratings are also built. Specifically, the principle of the magnification calibration method is expressed mainly by using two specific gratings with slightly different periods upper and down. The result would be a theoretical guideline for the magnification measurement and other design of Moiré-based metrological technique. Under the self-revised process, the accuracy of this method would be at the level of 0.4% with high sensitivity.

2. Principle

The principle of the interferometry approach can be explained by referring to Fig. 1. The light resource is first directed by a diaphragm, then uniformed and collimated through the collimation lens. At the incidence of planar wave, the diffraction waves of G_1 (referring composite grating

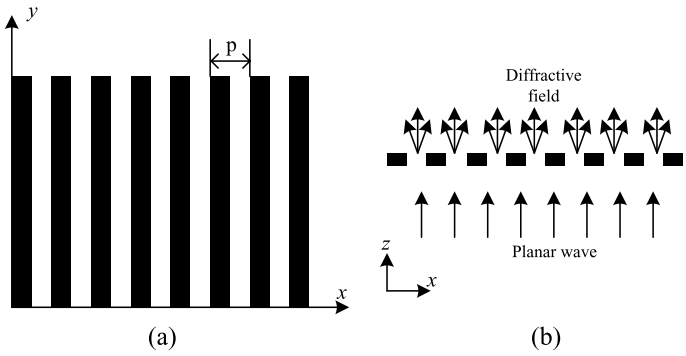

Fig. 2. (a) One-dimensional-grating with rectangular profile. (b) Diffraction model of 1-D-grating by planar wave.

mark) penetrate the BTLS which is expected to be calibrated, then interfere with mark G_2 (imaging composite grating mark) to generate Moiré fringes with two kinds of periods upper and lower which are collected by the following Charge Coupled Device (CCD) detector. Adopting Fourier-based phase analysis and phase unwrapping algorithm, different periods on the Moiré fringes could be precisely obtained for accurately evaluating the magnification [22]–[24].

Hereinafter, this paper briefly discusses the formation mechanism of Moiré for magnification calibration. As shown in Fig. 2(a), the period and duty circle of the 1D-grating with rectangular profile on x–y plane are respectively p and 1 : 1. According to Fourier Optics, the distribution of complex amplitude of diffractive wave in the plane close to the back of grating is related to its transmittance coefficient [25], [26].

Therefore, when the planar wave with amplitude E_0 travels through the 1-D-gratings, the complex amplitude of the diffractive wave can be decomposed as

$$E(x,y) = E_0 \cdot T_g(x,y) = E_0 \sum_{-\infty}^{+\infty} A_n \exp\left(i2\pi \frac{n}{p} x\right) \tag{1}$$

where $T_g(x,y)$ is transmittance coefficient of grating, A_n are the Fourier coefficient coefficients, n is the n_{th} diffractive order of gratings, and p is the period. According to (1), when planar wave transmits through the gratings, the consequence could be deemed as a superposition of different harmonics with discrete frequencies because of the periodicity of the gratings, as shown in Fig. 2(b).

Likewise we start with two standard 1-D-gratings, and the frequencies are assumed to be f_1 and f_2 where $f_k = 1/p_k (k = 1, 2)$. As was discussed before, the complex amplitude of the diffractive wave behind two gratings can, respectively, be expressed as

$$E_1(x,y) = E_0 \cdot T_1(x,y) = E_0 \sum_{-\infty}^{+\infty} A_n \exp(i2\pi n f_1 x) \tag{2}$$

$$E_2(x,y) = E_0 \cdot T_2(x,y) = E_0 \sum_{-\infty}^{+\infty} B_m \exp(i2\pi m f_2 x). \tag{3}$$

When the planar wave travels through these two superposed gratings, the amplitude of the diffractive wave behind the second grating can be written as

$$\begin{aligned} E(x,y) &= E_0 \cdot [T_1(x,y) \cdot T_2(x,y)] \\ &= E_0 \sum_{-\infty}^{+\infty} A_n \exp(i2\pi n f_1 x) \sum_{-\infty}^{+\infty} B_m \exp(i2\pi m f_2 x) \\ &= E_0 \sum_{(n,m)} A_n B_m \exp[i2\pi (n f_1 + m f_2) x] \end{aligned} \tag{4}$$

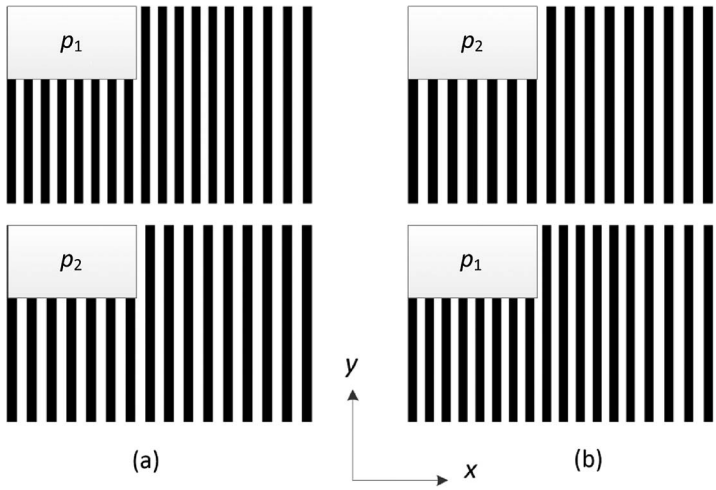

Fig. 3. (a) Referring grating mark G_1. (b) Imaging grating mark G_2, an up-down reverse of G_1.

where A_n and B_m are the Fourier coefficients. With the increase of diffraction order, the value of Fourier coefficient will decrease rapidly. The Moiré fringes are mainly generated by diffraction order 0 and ±1, the complex amplitude can be readily simplified as

$$E(x,y) = E_0 \cdot \left\{ \frac{1}{4} \sum_{-1}^{1} \sum_{-1}^{1} \text{sinc}\left(\frac{m}{2}\right) \text{sinc}\left(\frac{n}{2}\right) \exp[i2\pi(nf_1 + mf_2)x] \right\}$$
$$= E_0 \cdot \left\{ \frac{1}{4} + \frac{2}{\pi} [\cos(2\pi f_1 x) + \cos(2\pi f_2 x)] + \frac{2}{\pi^2} [\cos 2\pi(f_1 + f_2)x + \cos 2\pi(f_1 - f_2)x] \right\}. \quad (5)$$

Obviously, the Moiré fringes are mainly modulated by five different frequency components which contain 0, f_1, f_2, $(f_1 - f_2)$ and $(f_1 + f_2)$. Furthermore, when the periods of two grating marks are fairly close at the level of micrometer, the frequency difference is the most noticeable component under visible light which generates the most apparent periods on Moiré fringes [19], [27]–[29]. In addition, the consequence of superposing diffractive order (±1, ±1) is defined as the Moiré fringes; meanwhile, $(f_1 - f_2)$ is related to order (1, −1) and (−1,1). Thus, intensity of Moiré fringes can be simply expressed as (6), shown below, when neglecting the high-frequency components of grating mark

$$E_{(\pm1,\pm1)} = E_{(1,-1)} + E_{(-1,1)} = E_0 \cdot \left\{ A_1^2 \exp[i2\pi(f_1 - f_2)x] + A_1^2 \exp[i2\pi(f_2 - f_1)x] \right\}$$
$$= 2E_0 A_1^2 \cos(2\pi(f_1 - f_2)x) \quad (6)$$

where A_1 is the Fourier coefficient of the first diffractive order.

The periods of obtained Moiré fringes would be subsequently expressed as

$$p_{\text{moire}} = \frac{1}{|f_1 - f_2|} = \frac{p_1 \cdot p_2}{|p_1 - p_2|}. \quad (7)$$

Specifically, two composite grating marks are adopted in the approach. The referring grating mark G_1 is established with two 1-D linear gratings (Ronchi amplitude type), where the upper and lower parts are designed with slightly different periods. As shown in Fig. 3(a), the upper and lower periods of G_1 are chosen to be p_1 and p_2 respectively, while the imaging grating mark G_2 is determined by reversing the up-down of G_1, as shown in Fig. 3(b).

Due to the Talbot effect, the self-images of the grating p_1 and p_2 could reappear themselves at the distance $2kp^2/\lambda$ ($k = 1, 2, 3\ldots$), which is defined as the Talbot length [30]–[34], and p is the grating period while λ is the wavelength of the light. Superposing G_1 and G_2, the obvious

contrast of Moiré fringes are achieved by precisely adjusting the gap between G_1 and G_2 to a compromised value which keeps G_2 close to the Talbot distance [28], [35], [36].

In this paper, we first assume that the expected magnification (ρ) of BTLS is theoretically 1X; thus, the Moiré fringes formed by the interference of gratings display the same periods both upper and lower. Nevertheless, the actual value of magnification might not be extremely the designed value, and after the diffraction waves of G_1 transmit through BTLS, the deformed grating mark is imaged onto the second grating to form the Moiré fringes. Then, the period of grating G_1 is equivalently changed to be the corresponding periods p_1' which equals ρp_1. Therefore, the upper period of the finally obtained Moiré fringes could be described as

$$p_{\text{upper}} = \frac{p_1' \cdot p_2}{|p_1' - p_2|} = \frac{\rho \cdot p_1 \cdot p_2}{|\rho \cdot p_1 - p_2|} \tag{8}$$

where p_{upper} is the upper period of Moiré fringes, p_1 is the upper period of mark G_1, p_2 is the upper period of mark G_2, p_1' is the equivalent value of p_1 after diffraction waves transmit through BTLS, and ρ is the magnification of BTLS. As the same, the lower periods could similarly be presented as

$$p_{\text{lower}} = \frac{p_1 \cdot p_2'}{|p_1 - p_2'|} = \frac{p_1 \cdot \rho \cdot p_2}{|p_1 - \rho \cdot p_2|} \tag{9}$$

where p_{lower} is the lower period of Moiré fringes, p_2 is the lower period of mark G_1, p_1 is the lower period of mark G_1 and p_2' is the equivalent value of p_2.

It is evident that when magnification ρ is not exactly the designed value of 1X, the periods of the finally acquired consequence p_{upper} and p_{lower} will be totally different. Observing the value of p_{upper} and p_{lower}, we could find their numerator is the same while denominator is different because of the magnification ρ. For the differences between upper and lower, some intersections in the Moiré fringes would appear apparently.

Supposing both of the grating marks are fabricated with high accuracy (by the method of e-beam lithography), the periods of the referring grating G_1 and the imaging grating G_2 are exactly constant and precise. Benefiting from the intrinsic property of Moiré fringes, the obtained periods will be amplified when the values of p_1 and p_2 are fairly close according to Eq. (7). When there are some errors of the magnification in BTLS, the value of ρ could be obtained since p_1 and p_2 are already known meanwhile p_{upper} and p_{lower} will be acquired through a Fourier-based phase analysis algorithm after collecting the images by CCD detector. Furthermore, through calculating the average of both upper and lower consequences, this calibrating system could be more sensitive to the deviation of magnification.

3. Simulation

In order to confirm the accuracy of the proposed Moiré-based calibration method, two one-dimensional linear referring and imaging grating marks (both are Ronchi amplitude type) are generated in which the periods of G_1 are 6 μm and 6.6 μm up and down, respectively, while G_2 has a complementary arrangement with regard to G_1. With the purpose of checking effectiveness and accuracy of the proposed method, this paper has also completed the simulations of the whole calibrating process. For confirming the feasibility, we also add Gaussian white noises (mean noise of zero and variance of 0.1) to the consequences in the simulation, as shown in Fig. 4. It could be seen that the periods of upper and lower groups are definitely different resulted by the deviation of magnification.

For eliminating the noises and calculating the value of upper and lower periods, the phase of Moiré fringes at every corresponding position in x-direction is obtained by Fourier-based phase analysis. Initially, the obtained phase only ranges from $-\pi$ to π, which could results in an additional ambiguity in the wrapped phase map shown in Fig. 5(a) and (b). Additionally, with the purpose of calculating the continuous shape, a phase unwrapping algorithm is applied to eliminate

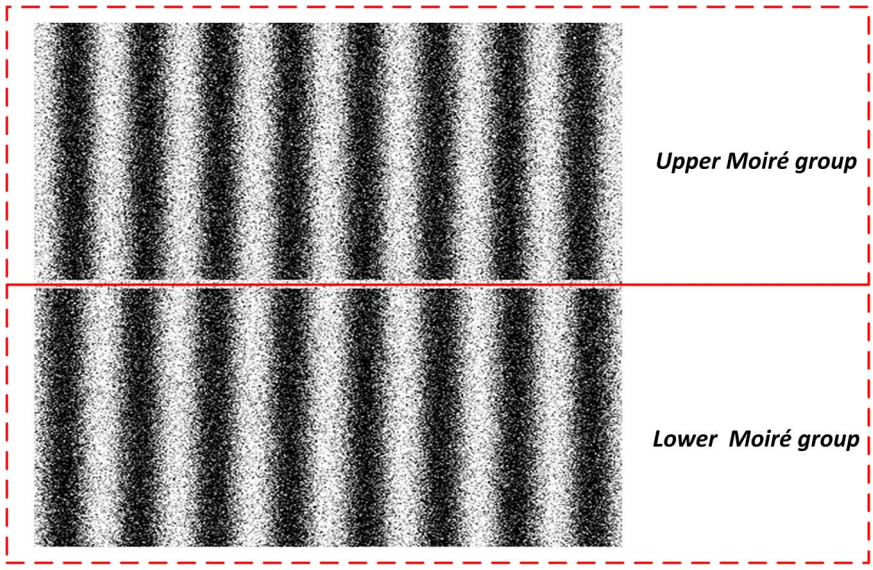

Fig. 4. Obtained Moiré fringes with different periods on upper and lower.

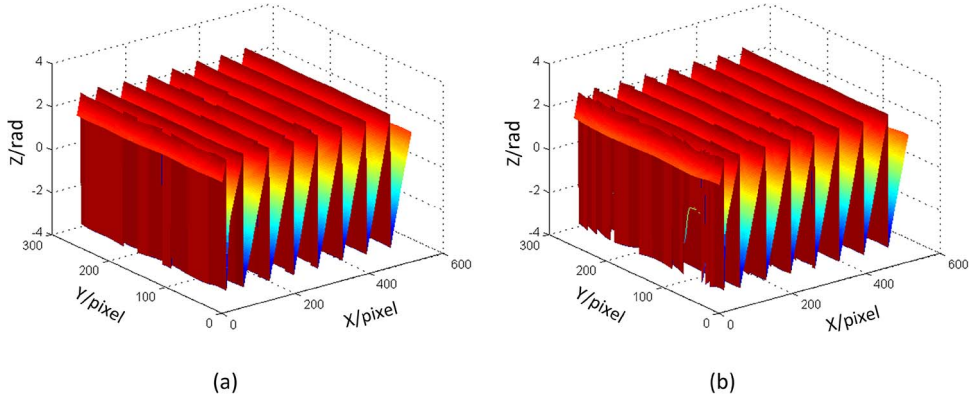

Fig. 5. (a) Wrapped phase of upper moiré fringes. (b) Wrapped phase of lower moiré fringes.

2π ambiguity, and the unwrapped shapes which have the usual smoothness of phase at every pixel are obtained, respectively, to increase the effectiveness, as shown in Fig. 6(a) and (b).

Furthermore, the phases of the Moiré fringes are proportional to the value of x after unwrapped according to (6), and it can be expressed as

$$\varphi_{\text{Moire}'} = ax + \varphi \tag{10}$$

where φ_{Moire} is the total phase of Moiré fringes, a is the slope of the continuously unwrapped phase by plotting the individual phases with respect to the corresponding pixels in x-direction, x is the initial position and φ is the original phase. As a consequence, through demodulating algorithms, we could initially evaluate the slope (a) of unwrapped phase. Therefore, by substituting the value of a into the equation $p = 2\pi/a$, the periods of upper and lower Moiré fringes could be calculated to be 65.641 μm and 66.343 μm respectively. By this method, the magnification could be theoretically evaluated to be 0.9993X according to (8) and (9). As the consequence is fairly close to the given value of 1X, the accuracy is evidently high enough with extraordinary sensitivity.

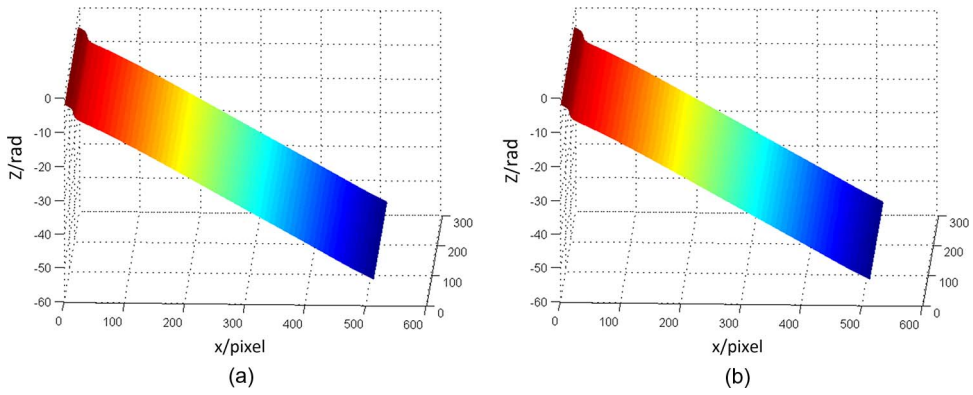

Fig. 6. (a) Unwrapped phase of upper moiré fringes. (b) Unwrapped phase of lower Moiré fringes.

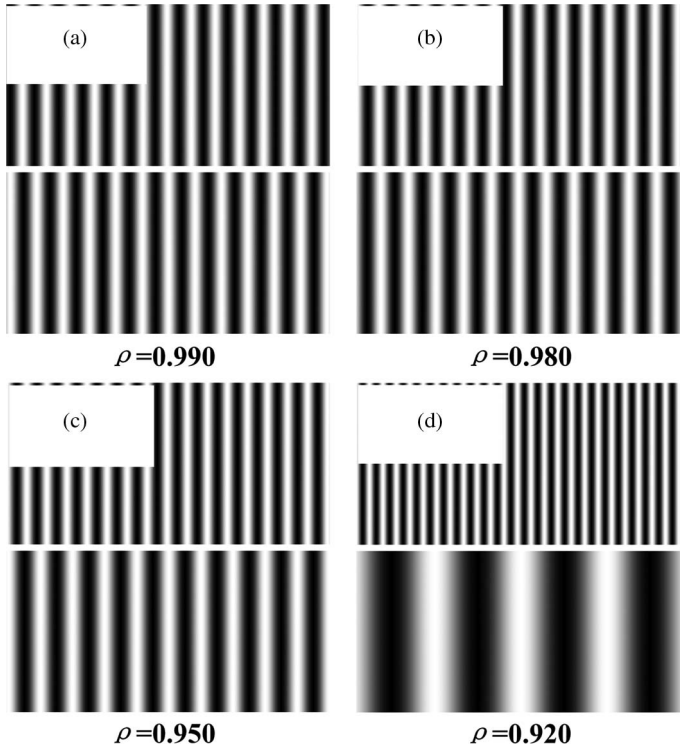

Fig. 7. Diagram of different Moiré fringes caused by different magnifications. (a) $\rho = 0.990$; (b) $\rho = 0.980$; (c) $\rho = 0.950$; (d) $\rho = 0.920$.

Certainly, the Moiré-based interferometry method also has the ability to calibrate the magnification with a wide range, making it easier to observe Moiré fringes when the exact magnification is far away from the designed value. Reasonably, due to the feature of the Moiré-based method, when magnification ρ is larger or smaller than the designed value 1X, the value of p_{upper} and p_{lower} will be totally different. Specially, according to (8) and (9), when the deviation is further away from the designed value, the differences between upper and lower periods will be more obvious, as shown in Fig. 7. Therefore, the proposed method could be more sensitive to calibrate the magnification.

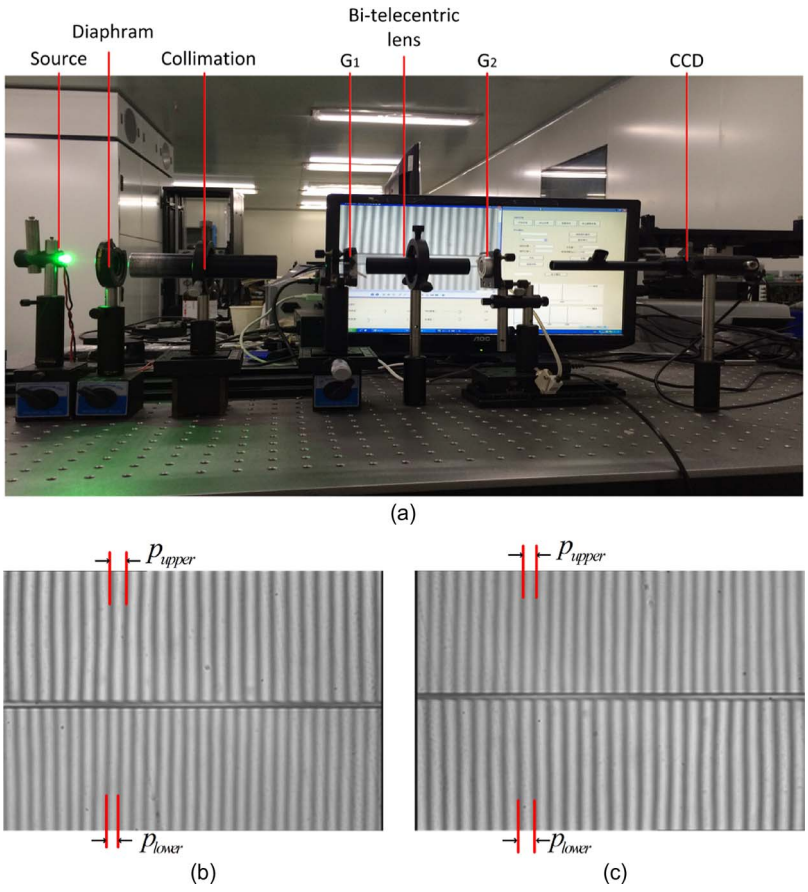

Fig. 8. (a) Experiment setup. (b) First obtained experimental Moiré fringes. (c) Another obtained moiré fringes after reversing the BTLS.

4. Experiment and Discussions

To experimentally verify the proposed method, an experimental system corresponding to the model described in Fig. 1 is established to evaluate the accuracy of magnification calibration, as shown in Fig. 8(a). The referring and imaging grating marks in experiment are fabricated by e-beam lithography, and the periods of p_1 and p_2 are produced to be 4 μm and 4.4 μm with almost negligible errors. The magnification of experimentally adopted BTLS is 1X with the inaccuracy less than 0.5%. The lighting source with wavelength of 633 nm illuminates the grating G_1 and penetrates through the BTLS; then, the deformed grating mark is imaged onto the second grating mark interfering with the imaging grating G_2. Finally, the Moiré fringes are real-time collected by a CCD detector (WAT902H, China) with imaging lens (NA $= 0.041$, Magnification $= 8\times$).

Since Talbot self images have a depth of focus, we need to confirm that the obtained Moiré fringes are clear enough. In addition, we also strictly regulate the optical path and adjust the gap between G_1 and G_2 to the Talbot distance. Before implementing the experiments, we try to move mark G_2 nearby the focus of Talbot self images, and the generated Moiré fringes are given in Fig. 8(b) and (c). With Fourier-based phase analysis and phase unwrapping algorithm mentioned in the simulation, the periods of p_{upper} and p_{lower} of Moiré fringes shown in Fig. 8(b) could be evaluated to be 48.266 μm and 40.728 μm, respectively. Finally, the magnification ρ_1 is calculated to be 1.0081X according to (8) and (9). The accuracy of this method would be influenced by the optical aberrations of the BTLS, the error of the periods in both grating marks, and the CCD pixel size. Although aberrations such as chromatic aberration and distortion

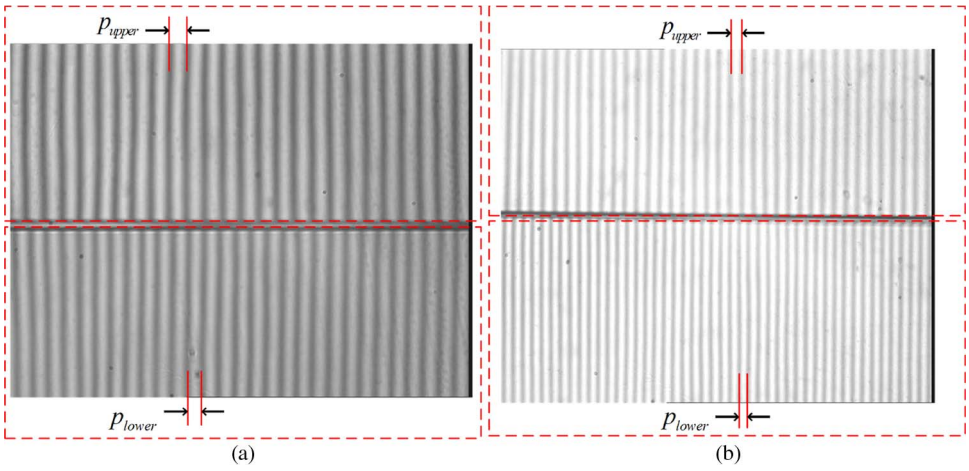

Fig. 9. (a) Experimental Moiré fringes of 2X. (b) Experimental Moiré fringes of 4X.

reduce the accuracy, they would have little influence on the effectiveness of this method when the applied fringes are linear. The proposed method adopts the Ronchi gratings and the final obtained fringes is linear, then the aberrations will have little influence on the accuracy [37]. Furthermore, if both periods of the gratings are identical with the same fabricating errors at nanometer, grating errors will also be of little importance [38].In the proposed method, the digitizing of the final image has to have influence in the Fourier analysis, and it is obvious that the smaller pixel size would make the calibration more precise, according to Shu [39].

Therefore, the accuracy is acknowledged to play a key role in the reliable calibration method. In addition, we also present an effective and simple self-revised process to check the calibrating error via reversing BTLS. Specifically, primarily carrying out the process and evaluating the magnification ρ_1 in the first step, we then reverse the BTLS to make the objective and imaging area of BTLS exchanged due to its intrinsic property. After exchanging objective and imaging area, we have subsequently obtained the new Moiré fringes, as shown in Fig. 8(c). The periods for upper and lower parts are respectively 38.814 μm and 50.083 μm with a similar magnification $\rho_2 = 0.9883$X. Although theoretical value ρ_2 could be the reciprocal of ρ_1, the actual magnification ρ_2 was not extremely the expected consequence on the account of calibrating error mentioned before. Therefore, this paper has described an effectively simple method to check the calibrating error defined as

$$\varepsilon = \frac{|\rho_2 - 1/\rho_1|}{\rho_2}. \tag{11}$$

As a consequence, the value of ρ_1 and ρ_2 are 1.0081X and 0.9883X respectively, the calibrating error could be calculated to be 0.37% according to the (11), which means that the accuracy of this proposed calibrating method is high enough to be suitable for calibrating BTLS applied recently [40], [41]. According to previous analysis, for evaluating the real value of magnification of BTLS, the key technology is to obtain the values of upper and lower periods of the final Moiré fringes meanwhile the whole calibrating system needs to be carefully constructed.

Although the analysis developed above is based on the hypothesis that the magnification of BTLS is theoretically 1X, the proposed method could also be widely used for any other value of magnification via analyzing the final obtained Moiré fringes. Moreover, in order to verify the accuracy of the proposed method at a wide range, the experiment is also conducted under other magnifications ranging from 1X to 4X, and the corresponding images are presented in Fig. 9.

Similarly, the results of magnification calibration are achieved as listed in Table 1 and the calibration errors are obtained by comparing the values of ρ_1 and ρ_2. Moreover, the designed

TABLE 1
The calibration results of different magnification of BTLS

Designed magnification	Calibration result (ρ_1)	Calibration result (ρ_2)	Calibration errors (ε)
1X	1.0081	0.9883	0.37 %
2X	2.0075	0.4996	0.29 %
4X	4.0110	0.2503	0.39 %

magnifications have no obvious influences on the calibrating errors, and the proposed Moiré-based method could keep a steadily high accuracy with a wide calibration range.

5. Conclusion

To make a conclusion, this paper proposes a Moiré-based interferometry method for calibrating the magnification of BTLS. Different from traditional methods, this method is simpler, faster, more precise and more sensitive to accomplish the calibration. Two precise grating marks with slightly different periods for upper and lower parts are respectively applied in the experiment, and Fourier-based phase analysis and phase unwrapping algorithm are adopted to evaluate the experimental Moiré fringes. Both simulation and experiment results have proved that the proposed approach has the capacity of achieving measurement accuracy up to 0.4%. Furthermore, the proposed method which is suitable enough for measuring the widely-used BTLS could also be applied in industry or laboratory.

Acknowledgment

The authors thank Y. Yang and Y. Tang for their helpful assistance during the experiment.

References

[1] J. S. Kim and T. Kanade, "Multiaperture telecentric lens for 3D reconstruction," *Opt. Lett.*, vol. 36, no. 7, pp. 1050–1052, Apr. 2011.
[2] M. Watanabe and S. K. Nayar, "Telecentric optics for focus analysis," *IEEE Trans. Pattern Anal. Mach. Int.*, vol. 19, no. 12, pp. 1360–1365, Dec. 1997.
[3] S. Luster, "Using telecentric lenses in inspection systems," *Vis. Syst. Des.*, vol. 10, no. 1, p. 28, Jan. 2005.
[4] A. E. Dixon, S. Damaskinos, A. R. And, and K. M. Beesley, "A new confocal scanning beam laser macroscope using a telecentric, F-theta laser scan lens," *J. Microscopy*, vol. 178, no. 3, pp. 261–266, Jun. 1995.
[5] K. H. Jin *et al.*, "Telecentric f-theta Lens for high-speed terahertz reflection three-dimensional imaging," in *Proc. IEEE 39th Int. Conf. IRMMW-THz*, 2014, pp. 1–2.
[6] J. G. R. Espino, J.-J. Gonzalez-Barbosa, R. A. G. Loenzo, D. M. C. Esparza, and R. Gonzalez-Barbosa, "Vision system for 3D reconstruction with telecentric lens," in *Proc. 4th Mexican Conf. Pattern Recog.*, 2012, pp. 127–136.
[7] X. Dai, H. Xie, C. Li, Z. Wu, and H. Geng, "High-accuracy magnification calibration for a microscope based on an improved discrete Fourier transform," *Opt. Eng.*, vol. 52, no. 11, pp. 1328–1342, Nov. 2013.
[8] E. F. Fullam, "Magnification calibration of the electron microscope," *J. Appl. Phys.*, vol. 14, no. 12, pp. 677–683, 1943.
[9] M. Reeves and G. Herriot, "SEM magnification calibration for metrology applications," in *Proc. SPIE*, 1989, pp. 46–55.
[10] C. Minwalla, E. Shen, P. Thomas, and R. Hornsey, "Correlation-based measurements of camera magnification and scale factor," *IEEE Sens. J.*, vol. 9, no. 6, pp. 699–706, Jun. 2009.
[11] R. Y. Tsai, "A versatile camera calibration technique for high-accuracy 3D machine vision metrology using off-the-shelf TV cameras and lenses," *IEEE J. Robot. Autom.*, vol. RA-3, no. 4, pp. 323–344, Aug. 1987.
[12] N. H. Olson, "Magnification calibration and the determination of spherical virus diameters using cryo-microscopy," *Ultramicroscopy*, vol. 30, no. 3, pp. 281–297, Jul./Aug. 1989.
[13] R. L. Read, "Assessment of on-screen measurements, magnification, and calibration in digital radiography," *J. Amer. Veterinary Med. Assoc.*, vol. 241, no. 6, pp. 782–787, Sep. 2012.
[14] D. De, "Moiré gauging of in-plane displacement using double aperture imaging," *Appl. Opt.*, vol. 11, no. 8, pp. 1778–1781, Aug. 1972.
[15] Y. Nakayama, J. Yamamoto, and H. Kawada, "Sub-50-nm pitch size grating reference for CD-SEM magnification calibration," *SPIE Adv. Lithography*, vol. 7272, pp. 1–11, Mar. 2009.
[16] J. A. van der Laak, H. B. Dijkman, and M. M. Pahlplatz, "Automated magnification calibration in transmission electron microscopy using Fourier analysis of replica images," *Ultramicroscopy*, vol. 106, no. 4/5, pp. 255–260, Mar. 2006.

[17] S. Zhou *et al.*, "Fourier-based analysis of moiré fringe patterns of superposed gratings in alignment of nanolithography," *Opt. Exp.*, vol. 16, no. 11, pp. 7869–7880, May 2008.
[18] S. L. Zhou, Y. Yang, L. X. Zhao, and S. Hu, "Tilt-modulated spatial phase imaging method for wafer-mask leveling in proximity lithography," *Opt. Lett.*, vol. 35, no. 18, pp. 3132–3134, Sep. 2010.
[19] S. Zhou *et al.*, "Moiré-based phase imaging for sensing and adjustment of in-plane twist angle," *IEEE Photon. Technol. Lett.*, vol. 25, no. 18, p. 1847, 2013.
[20] D. Post, "Moire interferometry for engineering and science," *Merida-DL Tentative*, vol. 5776, pp. 29–43, 2005.
[21] C. Di *et al.*, "A moiré-based four-channel focusing and leveling scheme for projection lithography," *IEEE Photon. J.*, vol. 6, no. 4, pp. 1–12, Aug. 2014.
[22] C. Di, W. Yan, S. Hu, D. Yin, and C. Ma, "Moiré-based absolute interferometry with large measurement range in wafer-mask alignment," *IEEE Photon. Technol. Lett.*, vol. 27, no. 4, pp. 435–438, Aug. 2015.
[23] H. Wang, "The Fourier analysis of Moire fringe," *J. Nanjing Univ. Sci. Technol.*, vol. 4, no. 1, pp. 70–74, Nov. 1991.
[24] A. S. D. Nicola, P. Ferraro, A. Finizio, and G. Pierattini, "Fourier transform method of fringe analysis for moire interferometry," in *Proc. SPIE*, 1999, vol. fc2, pp. 35–40.
[25] O. Bryngdahl and O. Bryngdahl, "Moire: Formation and interpretation," *J. Opt. Soc. Amer.*, vol. 64, no. 10, p. 1287, 1974.
[26] J. A. Quiroga, D. Crespo, and E. Bernabeu, "Fourier transform method for automatic processing of Moire deflectograms," *Opt. Eng.*, vol. 38, no. 6, pp. 974–982, 1999.
[27] K. Patorski, "Diffraction effects in moire deflectometry: Comment," *J. Opt. Soc. Amer. A, Opt. Image Sci.*, vol. 3, pp. 667–668, 1986.
[28] J. Zhu, S. Hu, P. Zhou, and J. Yu, "Experimental study of talbot imaging Moiré-based lithography alignment method," *Opt. Lasers Eng.*, vol. 58, pp. 54–59, 2014.
[29] H. Takasaki, "Moiré topography," *Appl. Opt.*, vol. 14, no. 1, p. 9, 1970.
[30] Y. Nakano and K. Murata, "Talbot interferometry for measuring the focal length of a lens," *Appl. Opt.*, vol. 24, no. 19, pp. 3162–3166, Oct. 1985.
[31] B. F. Oreb and R. G. Dorsch, "Profilometry by phase-shifted talbot images," *Appl. Opt.*, vol. 33, no. 34, pp. 7955–7962, Dec. 1994.
[32] M. V. B. S. Klein, "Integer, fractional and fractal talbot effects," *J. Modern Opt.*, vol. 43, no. 10, pp. 2139–2164, 1996.
[33] P. Cloetens, J. P. Guigay, C. De Martino, J. Baruchel, and M. Schlenker, "Fractional talbot imaging of phase gratings with hard X-rays," *Opt. Lett.*, vol. 22, no. 14, pp. 1059–1061, Jul. 1997.
[34] L. M. Sanchez-Brea, F. J. Torcal-Milla, and E. Bernabeu, "Talbot effect in metallic gratings under Gaussian illumination," *Opt. Commun.*, vol. 278, no. 1, pp. 23–27, Oct. 2007.
[35] K. Patorski, K. Pokorski, and M. Trusiak, "Circular-linear grating Talbot interferometry with moire Fresnel imaging for beam collimation," *Opt. Lett.*, vol. 39, no. 2, pp. 291–294, Jan. 2014.
[36] T. Sato, "Talbot effect immersion lithography by self-imaging of very fine grating patterns," *J. Vac. Sci. Technol. B, Microelectron. Process. Phenom.*, vol. 30, no. 6, 2012, Art. ID 06FG02.
[37] J. Buytaert, B. Ribbens, S. Vanlanduit, and J. J. J. Dirckx, "Aberration-free moire profilometry-analysis, simulation and implementation of the optimal setup geometry," *Opt. Lasers Eng.*, vol. 50, no. 8, pp. 1119–1129, Aug. 2012.
[38] D. W. Swift, "A simple moire fringe technique for magnification checking," *J. Phys. E, Sci. Instrum.*, vol. 7, pp. 164–166, 1974.
[39] Y. Shu and X. Wu, "Fourier analysis of high accurate detection based on image sensor CCD," *J. Exp. Mech.*, vol. 10, no. 1, pp. 31–37, 1995.
[40] C. L. Chang, K. C. Huang, W. H. Wu, and Y. H. Lin, "The design and fabrication of telecentric lens with large field of view," in Proc. *SPIE Opt. Eng. + Appl.*, 2010, pp. 197–325.
[41] H. Liao, Z. Chen, and X. Zhang, "Calibration of camera with small FOV and DOF telecentric lens," in *Proc. IEEE Int. Conf. ROBIO*, 2013, pp. 498–503.